Identification of Seawater Intrusion in the Dibdibba Coastal Aquifer, South of Iraq Using Chemical Indicators and Multivariate Analyses

Identification of Seawater Intrusion in the Dibdibba Coastal Aquifer, South of Iraq Using Chemical Indicators and Multivariate Analyses

Lamees S. Al-Qurnawy[1], Inass A. Almallah[2] and Aymen Alrubaye[3]

[1,3]Department of Sedimentology, Marine Science Center, University of Basrah, Basrah, Iraq.
[2]Department of Geology, College of Science, University of Basrah, Basrah, Iraq.

[1]E-mail: lamees.abdulhussein@uobasrah.edu.iq

Abstract. Seawater intrusion into the groundwater is a major environmental disaster which affects the environment as well as community. This research aims to analyze the seawater intrusion in the Dibdibba coastal aquifer. In this study, researchers used statistical techniques to examine the impact of seawater intrusion in the Dibddiba coastal aquifer in southern Iraq. They collected 15 groundwater samples from pumping wells during wet and dry periods and analyzed those using multivariate statistical analyses and ionic ratios based on the GIS technique. The results showed that there was a strong linear correlation between total dissolved solids (TDS) and several other ions, including $Ca^{2+,}$ $Mg^{2+,}$ $Na^{+,}$ $Cl^{-,}$ $SO^{-2}_{4,}$ and NO^{-3}. The principle component analysis revealed two factor loadings, with the first accounting for a significant portion of the total variance and showing a high loading for TDS, $Na^{+,}$ $Cl^{-,}$ $SO^{-2}_{4,}$ $Mg^{2+,}$ $Ca^{2+,}$ and NO^{-3}. The second factor had a high loading for K^{+}. The seawater influence was detected in 33.33 percent of the low zone groundwater, 26.66 percent of the moderate zone groundwater, and 40 percent of the high zone groundwater that was studied. Eighty and sixty-seven percent of the groundwater samples, respectively, belonged to the seawater field as Na-Cl type, as shown by Chadha's graphic, demonstrating the effect of seawater intrusion. Also, during the wet time, 20% of the samples belonged to the reverse ion exchange water field as Ca-Mg-Cl type, but during the dry period, 33.3% did. This is further evidence of the impact of seawater intrusion.

Keywords. Seawater intrusion, Aquifer, Multivariate analyses, Matrix, Ionic ratios, Ghadha.

1. Introduction

Seawater intrusion into the groundwater is a critical global issue that results in groundwater contamination. This threatens the environment, nature, and community. The problem is more crucial in arid and semi-arid regions in coastal areas where groundwater is the only supply source [1]. Seawater intrusion into unconfined aquifers could occur during tidal flooding followed by over-pumping, which reduces the groundwater table. The phenomenon is getting worse due to low recharge rates of groundwater owing to low rates of rainfall, which causes increasing salinization [2]. Seawater intrusion leads to various reactions which degrade groundwater quality and make it unfit for use. To name a few, oxidation and reduction reaction and ion exchange. These reactions alter the chemical composition of groundwater and thereby affect its quality [3].

Excessive use of groundwater lowers the water table. Besides this, anthropogenic activities such as releasing Greenhouse gases (GHGs) into the environment increase the carbon dioxide concentration, leading to rising sea levels. Lowering groundwater due to intensify agricultural practices such as large amounts of pumping and rising sea level significantly impact seawater intrusion [4]. Groundwater contamination by different sources degrades the water quality and is considered vulnerability [5]. Besides agricultural usages, biological processes release many pollutants into the air and water .These pollutants cause salinity and contaminate water with hazardous pollutants. The protection of environment and groundwater from the risk of aquifer vulnerability is an important responsibility that requires more decisions to create effective programs for protection [6].

The intrusion and the degree of vulnerability can be addressed if we know the source of salinity and discover affected wells that are exposed to the influence of seawater.

This research aims to analyze the seawater intrusion in the Dibdibba Coastal Aquifer using chemical indicators and multivariate analysis. To achieve this aim, following objectives have been devised:

- To measure the concentration of ions from different water samples in wet and dry season.
- To find the degree with which saltwater affect the groundwater.
- To assess the spatial distribution of ionic ratios for determining zones of seawater intrusion.

2. Material and Methods

2.1. The Study Area

The study area is located in the southeastern part of Basrah city south of Iraq, overlooks the marine coasts of the Arabian Gulf, and is situated between longitude 47˚39'0"E-47˚57'0"E and latitudes 30˚6'0"N-30˚18'0"N as Fig (1). It is bordered to the east by the Khor Al-Zubair estuary and Kuwait state to the direction of the south part. The area is significant as numerous wells feed the factories and agricultural lands. The drilled wells range from 10-25m in depth. The weather is hot and dry in the summer, whereas little rain is observed in winter. Hypersaline shallow water of the Khor al Zubair estuary is from the Arabian Gulf. Over 50 kilometers of water is the estuary length [7], and the breadth and depth are approximately 1-2 kilometers and 10-20 meters, respectively. Very high tides in the waterway can exceed 2.3 m [8].

Khor Al-Zubair and Umm Qasr are considered magnificent Iraq's largest ports; therefore, intensive activities such as trade occur there. Moreover, the major industrial and agricultural activities are fuelled through this coast [9].

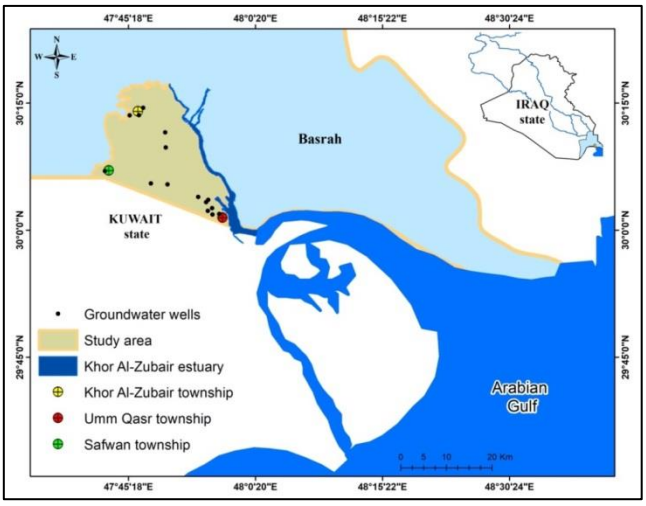

Figure 1. Location map of the study area displaying the groundwater wells.

2.2. Groundwater Sampling

Groundwater samples were taken from fifteen wells within areas of Khor Al-Zubair, Umm Qasr, and Safwan townships through wet and dry periods of 2021. The samples' electric conductivity (E.C.) was

tested in the field by WTW InoLab. The concentrations of eight major ions of water samples were tested according to chemical analyses procedures. Firstly, the Ca^{2+} concentration in water samples was measured by titration with EDTA (0.02 N) and Mg2+ by calculation. Na^{+} and K^{+} were calculated by Flame photometric method, Cl^{-} by titration based on Mohr method, SO^{-2}_{4} by Atomic Absorption spectrometer, HCO^{-}_{3} by titration method with HCl and minor ions NO^{-}_{3} by Prime Lab tool depends on wavelengths. The groundwater samples were tested in The Iraqi Group for the Science laboratory, and geochemical laboratory," affiliated with the Marine Science Center/the University of Basrah, and Quality Control laboratory affiliated with the Basrah water Directorate.

2.3. Ionic Ratios

The concentration of ions in water samples was used to identify the saline and freshwater zones in the coastal aquifers. Seawater contamination can be assessed using chemical data, analyzing major ion concentrations, and correlating them with total dissolved solids [10]. Similarly, ionic ratios can help determine groundwater source in coastal areas in relevance to chloride ions [11]. It is worth noting that ionic ratios are used to detect marine intrusion and to understand other processes impacting groundwater chemistry, such as water-rock interaction [12]. Seawater typically contains high levels of chloride and sodium, and elevated concentrations of these ions in coastal areas may indicate a mixing process with groundwater. However, some components of saltwater are commonly overlooked because of the change and conversion that occurs when seawater interacts with aquifer sediments [13]. Chloride and total dissolved solids levels that are abnormally high in wells located near the shore may be an indication of saltwater intrusion [14]. In ArcGIS software, inverse distance weighted interpolation (IDW) and overlay techniques can be used to generate spatial distribution maps of ionic ratios and assess the trend of salinity [3].

2.4. Chadha's Diagram

Ghadha designed this diagram in 1999 to interpret and explain the hydrochemical process, which is responsible for assessing the quality and origin of groundwater [15]. The diagram is significant in detecting seawater intrusion besides water-rock interaction in coastal aquifers [16]. Chadha's plot can be categorized into eight zones in Fig (2) next [17]:

- Alkaline earth exceeds alkali metals.
- Alkali metals exceed alkaline earth.
- Weak acidic anions exceed strong acidic anions.
- Strong acidic anions exceed weak acidic anions.
- Alkaline earth and weak acidic anions exceed alkali metals and strong acidic anions.
- Alkaline earth exceeds alkali metals, and strong acidic anions exceed weak acidic anions.
- Alkali metals exceed Alkaline earth, and strong acidic anions exceed weak acidic anions.
- Alkali metals exceed alkaline earth, and weak acidic anions exceed strong acidic anions.

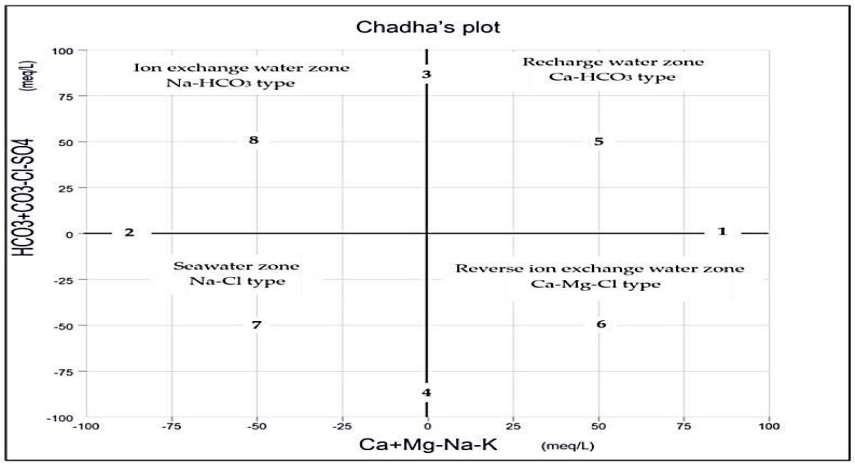

Figure 2. Chadha's diagram for groundwater types.

2.5. Data Analysis

The relative difference of the water sample (n = 15) was calculated first to check whether the samples could help achieve the research objectives. The statistical package for social sciences (SPSS) software was used as an effective tool for data analysis. Descriptive and inferential statistics were applied to find the trends in the dataset.

3. Results and Discussion

3.1. Analysis of Data Accuracy by Relative Differences %(R.D)

The degree to which a measured quantity corresponds to its true value is known as its accuracy. As shown in (Equation 1), accuracy in performance has been achieved by employing the law of ion equilibrium (Cations-Anions) proposed by [18].

$$R.D= (\sum|Cations|-\sum Anions|)/(\sum|Cations|+\sum Anions|)\times 100 \quad (1)$$

The relative difference (R.D.) value was calculated for 15 water samples. The results indicate that 66.66% of samples have good data quality within. In contrast, about 23.33% of samples have acceptable data quality having R.D. value ranges between 5-10%, and about 10% of samples have poor data quality as they scored more than 10 % R.D.

From the results, it is assumed that data is good to achieve the research objectives. Table 1 showed the descriptive statistical analysis for the groundwater sample.

Table 1. Descriptive statistical analysis of sampled groundwater for the two periods.

Parameters	Wet period				Dry period			
	Min	Max	Mean	S.D	Min	Max	Mean	S.D
Ca^{2+} (mg/l)	395	842	545	151	381	1274	677	312
Mg^{2+} (mg/l)	239	507	329	92	230	770	407	189.7
Na^{+} (mg/l)	298	3725	1841	1102	301	3663	1944	1125
K^{+} (mg/l)	11.4	86	22	18	6.1	41.9	12.87	8.6
Cl^{-} (mg/l)	595.6	4766	2226	1323	595.5	4634	2414	1420.4
SO_4^{-2} (mg/l)	1732.4	3888.5	2847	699	1693	6128	3152.6	1556.7
HCO_3^{-} (mg/l)	103.7	433	232.6	94	91.5	451.4	228	101.8
NO_3^{-} (mg/l)	0.48	1.23	0.85	0.3	0.62	1.76	1.25	0.43
TDS (mg/l)	3156	12103.5	7488.1	3069	2956.8	12929	7931	3426.85
pH	6.95	7.25	7.14	0.01	7.08	7.79	7.36	0.196
EC (µS/Cm)	4931	18911.7	11700	4795.6	4620	20200	12392	5354.5

3.2. Multivariate Statistical Analyses

Multivariate statistical analysis examines data to identify relationships between variables that were not previously known. It is commonly used to analyze groundwater chemistry [19] and can involve techniques such as principal component analysis (also known as factor analysis) [20]. This method helps to reduce the amount of data by identifying the most important variables while minimizing the loss of information. This makes it easier to interpret the correlation between different parameters [17]. The main goal of using multivariate statistical analysis is to simplify and interpret complex data to better understand the parameters being evaluated [21].

3.2.1. Correlation Coefficient Matrix

Often used to analyze the relationship between two variables is the correlation coefficient matrix. It helps to assess the predictive power of one variable based on another [22]. When the correlation coefficient is close to 1 or -1, it indicates a strong correlation between the variables, while a value close to zero indicates a weak correlation. In this the study, the chemistry of groundwater was analyzed by examining nine variables, including Ca^{2+}, Mg^{2+}, Na^{+}, K^{+}, Cl^{-}, HCO_3^{-}, SO_4^{2-}, NO_3^{-}, and TDS. Tables 2 and 3 show the relationship between these factors during both rainy and dry times, respectively. TDS displayed a strong positive association with Ca2+, Mg2+, Na+, Cl, SO24, and NO3 during the wet period, indicating that these cations all originated from the same place and were

subjected to the same processes (such as seawater intrusion, water-rock interaction, and ion exchange) during this time. Nevertheless, TDS had only a moderate positive connection with K+ and a moderate negative correlation with HCO_3. An excellent positive association was found between TDS and Na^+, Cl, and NO_3 during the dry period; a very good positive correlation was found between TDS and Ca^{2+}, Mg^{2+}, and SO^2_4; and a poor correlation was found between TDS and K+ and HCO_3 during the same time period. As Na^+ and Cl tend to be found together, this might indicate the existence of halite or seawater intrusion, and the presence of both Na+ and Cl in groundwater would point to the dissolution of halite [19]. Since the concentration of Cl^- is higher than Na+ in the sampled groundwater; increasing salinity is likely due to seawater intrusion.

Table 2. Parameter-setting wet-season correlation matrix.

	Parameters	**Ca^{2+}**	**Mg^{2+}**	**Na^+**	**K^+**	**Cl^-**	**SO^2_4**	**HCO_3**	**NO_3**	**TDS**
Correlation	Ca^{2+}	1.000								
	Mg^{2+}	1.000	1.000							
	Na^+	.986	.985	1.000						
	K^+	.004	.004	.006	1.000					
	Cl^-	.984	.983	.993	-.004	1.000				
	SO^{-2}_4	.959	.959	.974	-.060	.969	1.000			
	HCO_3	-.209	-.208	-.175	.052	-.206	-.169	1.000		
	NO^-_3	.920	.918	.953	.002	.972	.923	-.219	1.000	
	TDS	.987	.986	.996	.011	.996	.980	-.168	.954	1.000

Bold values strong significant correlation at 0.01 levels.

Table 3. Parameter-setting dry-season correlation matrix.

	Parameters	**Ca^{2+}**	**Mg^{2+}**	**Na^+**	**K^+**	**Cl^-**	**SO^2_4**	**HCO_3**	**NO_3**	**TDS**
Correlation	Ca^{2+}	1.000								
	Mg^{2+}	1.000	1.000							
	Na^+	.841	.839	1.000						
	K^+	.172	.173	.221	1.000					
	Cl^-	.827	.825	.995	.260	1.000				
	SO^{-2}_4	.997	.997	.851	.177	.833	1.000			
	HCO_3	-.039	-.037	-.151	-.323	-.160	-.042	1.000		
	NO^-_3	.666	.663	.950	.273	.967	.671	-.193	1.000	
	TDS	.858	.856	.998	.261	.995	.867	-.146	.943	1.000

Bold values strong significant correlation at 0.01 levels.

3.2.2. KMO and Bartlett's Test

To determine if the data is suitable for factor analysis, measures of sampling data adequacies such as Kaiser-Meyer- Olkin and Bartlett's test are used. A KMO score of at least 0.6 is considered adequate for performing factor analysis **[23]**. Table (4) shows the results of these tests for the wet and dry periods. The KMO scores are 0.77 and 0.66, respectively, which indicates good data adequacy. Another indicator that the data is appropriate for principal component analysis is the outcome of the Bartlett's test, which yields degrees of freedom of 354.14 and 401.7 for the wet and dry periods, respectively, at a significance level of less than 0.05 for both periods.

Table 4. KMO and Bartlett's test at wet and dry periods.

Kaiser-Meyer-Olkin Measure of Sampling Adequacy.		**Wet period .769**	**Dry period .659**
Bartlett's Test of Sphericity	Approx. Chi-Square	354.144	401.682
	df	36	36
	Sig.	.000	.000

3.2.3. Eigen Values and Total Variance of Components

The important factor loadings between variables are considered to interpret the factors obtained through factor analysis. The eigenvalue is a measure of the significance of a factor, with factors having eigenvalues greater than one is more significant. Factor loadings are classified as weak (0.30-0.50),

moderate (0.50-0.75), or strong (up to 0.75) based on their absolute loading values [17]. Factors with less than one eigenvalues and those close to zero can be neglected [19]. In the study area, Tables (5) and (6) show the eigenvalues, percentages of the total variance, and cumulative variance of principal components for the hydrochemical parameters during the wet and dry periods. During the rainy phase, we received two principal components as factor loadings with eigenvalues of roughly (6.87) and (1.00), while during the dry period, we obtained two principal components with eigenvalues of approximately (6.36) and (1.3). When figuring out the chemical make-up of groundwater, the major considerations are the components with high eigenvalues (6.87 and 6.36).

Table 5. Eigen values and total variance explained for wet period.

Component	Initial Eigenvalues			Extraction Sums of Squared Loadings			Rotation Sums of Squared Loadings		
	T	V %	C %	T	V%	C %	T	V%	C %
1	6.868	76.306	76.306	6.868	76.306	76.306	6.807	75.633	75.633
2	1.036	11.508	87.815	1.036	11.508	87.815	1.096	12.182	87.815
3	.927	10.299	98.114						
4	.110	1.221	99.335						
5	.048	.537	99.871						
6	.008	.091	99.963						
7	.003	.030	99.993						
8	.001	.007	100.000						
9	3.605E-5	.000	100.000						

Extraction Method: Principal Component Analysis.

Where, T is total, V is variance, C is cumulative.

Table 6. Eigen values and total variance explained for dry period.

Component	Initial Eigenvalues			Extraction Sums of Squared Loadings			Rotation Sums of Squared Loadings		
	T	V %	C %	T	V %	C %	T	V %	C %
1	6.358	70.650	70.650	6.358	70.650	70.650	6.201	68.899	68.899
2	1.309	14.549	85.199	1.309	14.549	85.199	1.467	16.300	85.199
3	.692	7.685	92.884						
4	.621	6.899	99.783						
5	.017	.187	99.970						
6	.001	.016	99.986						
7	.001	.012	99.998						
8	.000	.002	100.000						
9	1.492E-5	.000	100.000						

Extraction Method: Principal Component Analysis.

3.2.4. Factor Loadings

To summarize, Table (7) displays the results of the principal component analysis for both wet and dry periods. Two factors were identified for each period, with eigenvalues up to 1. Factor (1) had high positive loadings for several components, including TDS, Na^{+}, Cl^{-}, Ca^{2+}, Mg^{2+}, SO^{2}_{4}, and NO_{3}, which accounted for 76.306% and 70.650% of total variance for the wet and dry periods, respectively. Factor (2) had high positive loadings for K^{+} and accounted for 11.508% and 14.549% of the total variance for the wet and dry periods, respectively. The strong positive loadings among Na^{+}, Cl^{-}, and TDS indicated the influence of seawater on the aquifer particularly due to the conservative behavior of chloride ions [11]. High concentrations of Cl^{-} up to 1000 mg/l in groundwater near coastal areas may indicate seawater intrusion, which can be caused by factors such as salinization, sea spray, and septic sources [3]. Components with high factor loadings up to 0.5 in relation to Na^{+}, Cl^{-}, Mg^{2+}, and SO^{2}_{4} are likely seawater ions [24].

Table 7. Varimax rotated factor analysis of parameter set at wet and dry periods.

Parameters	Component for Wet		Parameters	Component of Dry	
	1	2		1	2
TDS	.997	-.055	TDS	.965	.196
Na^+	.994	-.062	Na^+	.959	.185
Cl^-	.994	-.087	SO^{-2}_4	.952	-.021
Ca^{2+}	.986	-.082	Cl^-	.950	.220
Mg^{2+}	.986	-.081	Ca^{2+}	.948	-.028
SO^{-2}_4	.971	-.115	Mg	.947	-.029
NO^-_3	.957	-.090	NO	.849	.303
K^+	.079	.850	HCO3	-.007	-.824
HCO3	-.171	.569	K^+	.149	.757
Extraction Method: Principal Component Analysis.					
Rotation Method: Varimax with Kaiser Normalization.					

3.3. Ionic Ratios

The purpose of this study was to investigate the spatial distribution of five ionic ratios in milliequivalent per liter, including Na^+/Cl^-, HCO_3/Cl^-, Mg^{2+}/Cl^-, SO_4/Cl^-, and K^+/Cl^-. The spatial distribution mapping was conducted using ArcGIS v.10.3 to assess the zoning of seawater intrusion. In order to reclassify the ranges of ionic ratios data, an interpolation process was employed using Inverse Distance Weighted (IDW) as noted by [3]. The maps were then reorganized by category. In GIS, we used the Weighted Overlay Spatial Analyst to combine the ionic ratio maps from both time periods into a single cohesive whole. The ionic ratios' descriptive statistics are shown in Table (8).

Table 8. Descriptive statistical analysis of ionic ratios for the two periods

Chemical indicator	Wet period				Dry period			
	Mean	Min	Max	S.D	Mean	Min	Max	S.D
Na^+/Cl^-	1.26	0.65	1.72	0.32	1.24	0.78	1.75	0.27
Cl^-/HCO_3	18.67	5.45	53.7	13.4	20.4	5.28	50.20	12.82
Mg^{2+}/Cl^-	0.55	0.31	1.17	0.27	0.61	0.34	1.17	0.21
SO_4/Cl^-	1.20	0.54	2.18	0.51	1.19	0.79	2.21	0.37
K^+/Cl^-	0.013	0.003	0.04	0.01	0.01	0.002	0.02	0.005

3.3.1. Na/Cl

To determine the presence of seawater intrusion in wells, the Na^+/Cl^- ratio is commonly used. High levels of chloride and sodium ions characterize marine water. A ratio of Na^+/Cl between 0.86-1 (molar ratio) in groundwater indicates that seawater has influenced it [25]. If the ratio exceeds 1, it may indicate contamination from anthropogenic sources [26]. A ratio less than 0.86 indicate seawater intrusion [27]. The spatial distribution of Na^+/Cl^- in the study area ranged from 0.65-1.72 and 0.78-1.75 in wet and dry periods, respectively, as shown in Fig. 3(a) and (b). The lower end of the range suggests a high likelihood of seawater influence.

3.3.2. Cl^- / HCO_3

To evaluate the impact of seawater on the groundwater, Simpson's index is a magnificent ratio [28], according to [1]. This index categorizes the level of water contamination into six levels, as suggested by [29]. Good water has an index of equal to or less than 0.5, slightly contaminated water ranges from 0.5 to 1.3, moderately contaminated water ranges from 1.3 to 2.8, injuriously contaminated water ranges from 2.8 to 6.6, highly contaminated water ranges from 6.6 to 15.5, and severely contaminated water has an index of above 15.5 with seawater intrusion.

The spatial distribution of Cl^- / HCO_3 ranged from 5.45-53.7 and 5.28-50.20, as shown in Fig.3 (c) and (d) respectively. High ranges indicate a high effect of seawater mixing in these areas.

3.3.3. Mg^{2+}/Cl^-

When dolomite dissolves and silicate minerals weather, it can increase the concentration of Mg2+ in groundwater. High levels of Mg2+ are an indication of seawater intrusion [30]. The spatial distribution of Mg^{2+}/Cl^- ranged from 0.31 to 1.17 for both wet and dry periods, as illustrated in Fig. 3(e) and (f). Low values in this ratio indicate a high impact on seawater mixing.

3.3.4. SO^2_4/Cl^-

To determine seawater intrusion, the ratio of SO^2_4 to Cl^- is important. If the ratio is less than 1, it indicates seawater intrusion due to the dominance of Cl^- over SO^2_4 [1]. If the ratio exceeds 1, it could be due to the use of gypsum fertilizers [14], or the dissolution of gypsum [31]. The spatial distribution of SO^2_4/Cl^- ratios ranged from 0.54 to 2.18 and 0.79 to 2.21, as shown in Fig.3 (g) and (h). Low ratios in an area indicate a high effect of seawater intrusion.

3.3.5. K^+/Cl^-

According to [26], the K^+/Cl^- ratio in groundwater tends to decrease in the presence of seawater contamination due to the absorption of potassium ions by clay deposits. The spatial distribution of K^+/Cl^- ranged from 0.003-0.04 and 0.002-0.02, as shown in Fig5. (i) and (j), respectively. Areas with low ranges indicate a high level of seawater intrusion.

3.4. Extracted Final Map

Figure 3(k) and (l) show the final combined maps, which distinguish between low, moderate, and high seawater effect zones. Around 33.33 percent of the groundwater samples come from the low-impact zone, which is primarily located in wells in the northern portion of Khor Al-Zubair and a few wells in the southern parts of Umm Qasr. It was found that 26.66 percent of the groundwater samples were located in the moderate impact zone. Wells in the south of Umm Qasr, the southeast of Khor Al-Zubair, and the southwest between Umm Qasr and Safwan are located in the high impact zone, which accounts for 40% of the analyzed groundwater.

3.5. Chadha's diagram

Figures (4) and (5) show the conditions of high groundwater salinity on Chadha's plot, plotted in milliequivalents per liter. The sampled groundwater during the wet and dry periods had 80% and 66.7%, respectively, belonging to the Na-Cl water type within the seawater domain. This is shown in (Zone 7) of the plot, where alkali metals exceed alkaline earth and strong acidic anions exceed weak acidic anions. About 20% and 33.3% of the samples for the same periods were under the Ca-Mg-Cl water type (Zone 6), which is under the inverse ion exchange zone, indicating that alkaline earth exceed alkali metals and strong acidic anions exceed weak acidic anions. High ratios of Na-Cl type showed that seawater intrusion had an effect during both time periods.

Seawater intrusion in coastal aquifers is related to reverse ion exchange, dissolution, and precipitation processes, as stated in [1]. Due to low seasonal rainfall and recharge water, none of the samples were found in the recharge water zone ($Ca\text{-}HCO_3$).

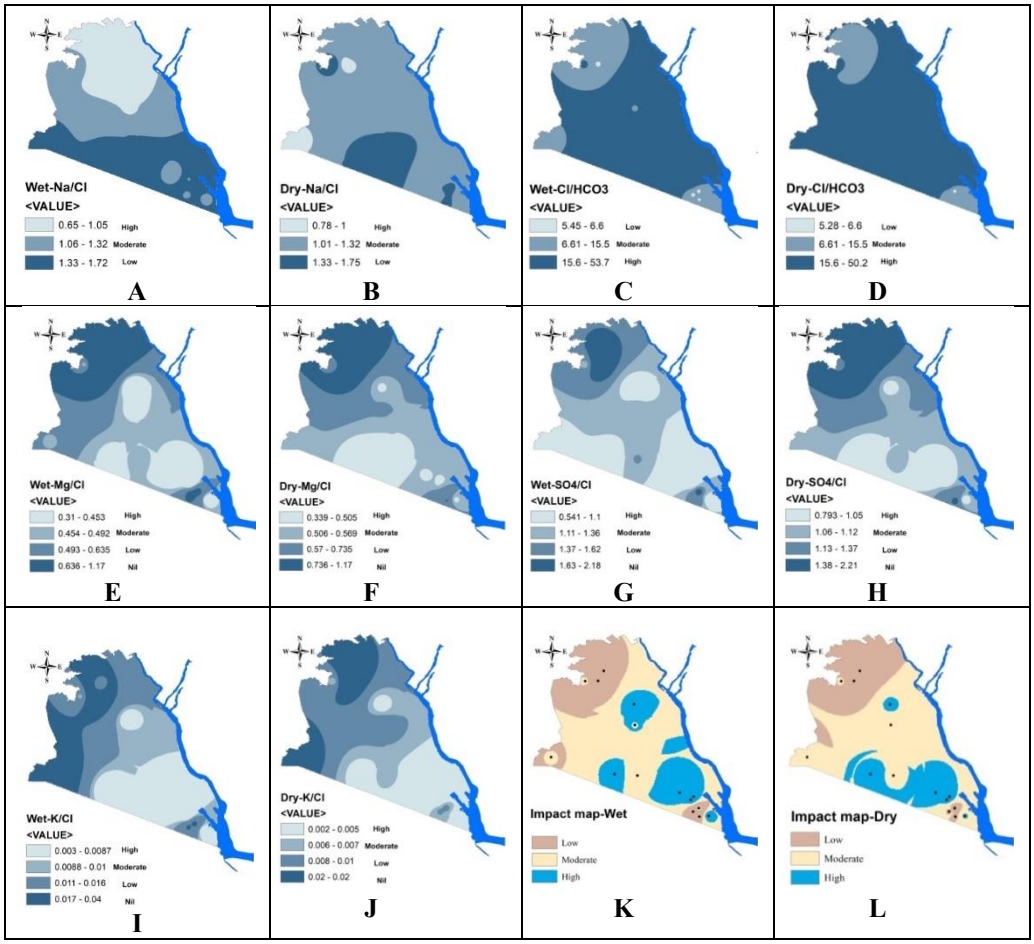

Figure 3. Spatial distribution of ionic ratios and extracted impact maps.

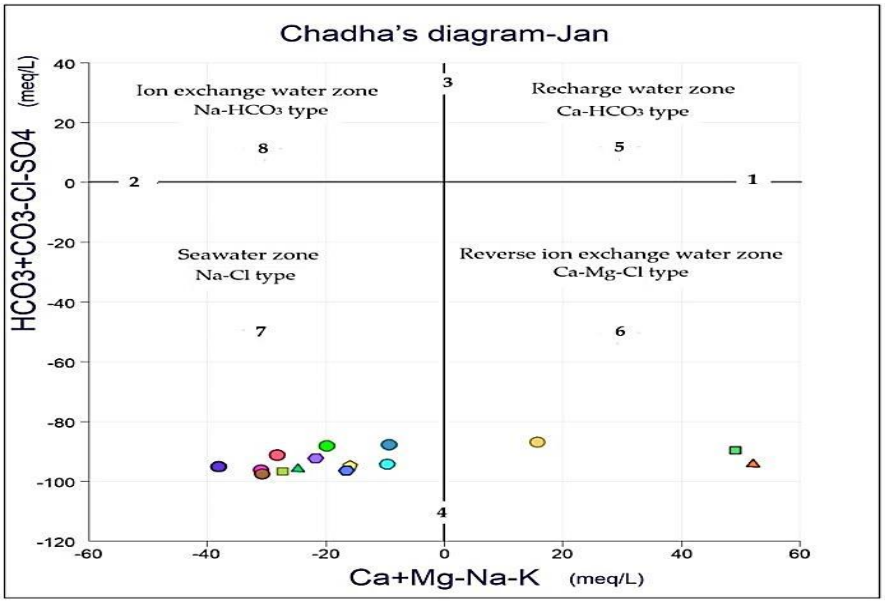

Figure 4. Chadha's diagram of groundwater samples for wet season.

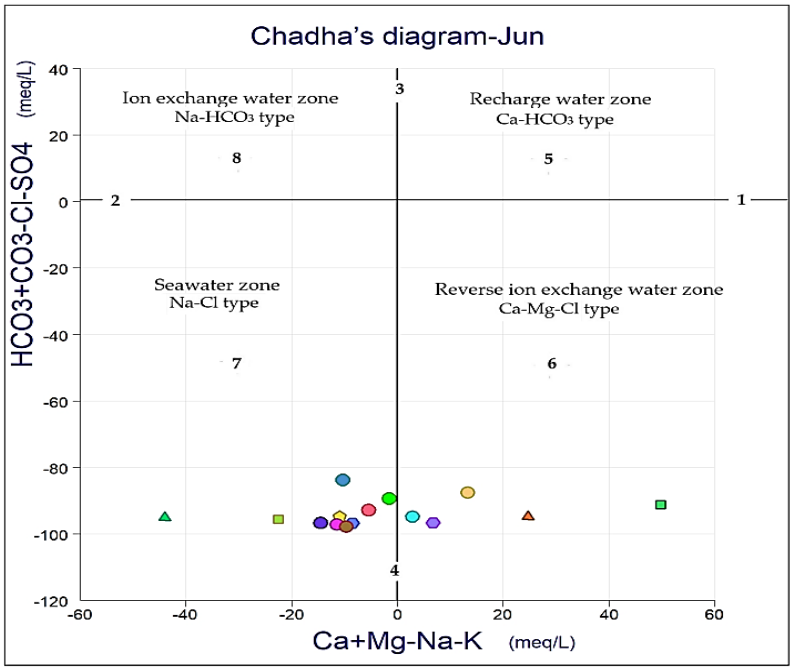

Figure 5. Chadha's diagram of groundwater samples for dry season.

Conclusion

Ca^{2+}, Mg^{2+}, Na^{+}, Cl, SO_2^4, and NO_3 showed strong linear correlations with TDS in both time periods, suggesting they are related. Due to its considerably positive loadings across components TDS, Na^{+}, Cl^{-}, Ca^{2+}, Mg, SO_2^4, and NO^{-3}, Factor 1 (PCA1) in the principal component analysis explained 76.306% and 70.650% of the overall variation during the wet and dry periods, respectively. Positive K^{+} loadings dominated PCA factor 2, explaining 11.508 and 14.549 percent of the variation during the wet and dry periods, respectively. Positive factor loadings for salt, chloride, and total dissolved solids indicate seawater effect on the aquifer.

To clarify, 40% of the sampled groundwater in the study area showed a strong impact of seawater intrusion, with wells in the wet period being more affected than those in the dry period. Approximately 26.66% of the wells showed a moderate impact, while 33.33% showed a low impact.

In terms of Chadha's diagram, 80% of the groundwater samples in the wet period and 66% in the dry period fell within the seawater zone (NaCl) type, indicating a strong impact of seawater intrusion. The remaining wells (20% and 33.3% in the wet and dry periods, respectively) were located within the reverse ion exchange water zone, which is also related to seawater intrusion.

References

[1] Abdalla, F. (2016). Ionic ratios as tracers to assess seawater intrusion and to identify salinity sources in Jazan coastal aquifer, Saudi Arabia. Arabian Journal of Geosciences, 9(1), 1-12.

[2] Naily, W. (2018, February). Ratio of major ions in groundwater to determine saltwater intrusion in coastal areas. In IOP conference series: earth and environmental science (Vol. 118, No. 1, p. 012021). IOP Publishing.

[3] Asare, A.; Appiah-Adjei, E. K.; Ali, B. and Owusu-Nimo, F. (2021). Assessment of seawater intrusion using ionic ratios: the case of coastal communities along the Central Region of Ghana. Environmental Earth Sciences, 80(8), 1-14.

[4] Alqurnawy, L. S.; Almallah, I. A. and Alrubaye, A. (2022). Groundwater Vulnerability Analysis via GALDIT-GIS Method to Seawater Intrusion, South of Iraq. The Iraqi Geological Journal, 146-161.

[5] Al-Abadi, A. M.; Al-Shamma'a, A. M. and Aljabbari, M. H. (2017). A GIS-based DRASTIC model for assessing intrinsic groundwater vulnerability in northeastern Missan governorate, southern Iraq. Applied Water Science, 7(1), 89-101.

[6] Al-Abadi, A. (2021). Groundwater Vulnerability Evaluation in the Nineveh Plain, Northern Iraq, using a GIS-based DRASTIC Model. Iraqi National Journal of Earth Sciences, 21(2), 78-92.

[7] Sissakian, V. K.; Abdul Ahad, A. D.; Al-Ansari, N. and Knutsson, S. (2018). Neotectonic activity from the upper reaches of the Arabian Gulf and possibilities of new oil fields. Geotectonics, 52(2), 240-250.
[8] Dakheel, A. A.; Al-Aboodi, A. H. and Abbas, S. A. (2022). An empirical formula development to predict suspended sediment load for Khour Al-Zubair port, South of Iraq. Open Engineering, 12(1), 169-175.
[9] Al-Suraifi, A. A. A. (2015). Groundwater and Seawater Intrusion Simulation at Basrah Coastal Aquifer. In The 2 nd International Conference of Buildings, Construction and Environmental Engineering (BCEE2-2015) (p. 63).
[10] Lee, J. Y. and Song, S. H. (2007). Groundwater chemistry and ionic ratios in a western coastal aquifer of Buan, Korea: implication for seawater intrusion. Geosciences Journal, 11(3), 259-270.
[11] Arslan, H. (2013). Application of multivariate statistical techniques in the assessment of groundwater quality in seawater intrusion area in Bafra Plain, Turkey. Environmental monitoring and assessment, 185(3), 2439-2452.
[12] Kura, N. U.; Ramli, M. F.; Ibrahim, S.; Sulaiman, W. N. A. and Aris, A. Z. (2014). An integrated assessment of seawater intrusion in a small tropical island using geophysical, geochemical, and geostatistical techniques. Environmental Science and Pollution Research, 21(11), 7047-7064.
[13] Seddique, A. A.; Masuda, H.; Anma, R.; Bhattacharya, P.; Yokoo, Y. and Shimizu, Y. (2019). Hydrogeochemical and isotopic signatures for the identification of seawater intrusion in the paleobeach aquifer of Cox's Bazar city and its surrounding area, south-east Bangladesh. Groundwater for Sustainable Development, 9, 100215.
[14] Ghabayen, S. M.; McKee, M. and Kemblowski, M. (2006). Ionic and isotopic ratios for identification of salinity sources and missing data in the Gaza aquifer. Journal of hydrology, 318(1-4), 360-373.
[15] Chadha, D. K. (1999). A proposed new diagram for geochemical classification of natural waters and interpretation of chemical data. Hydrogeology journal, 7(5), 431-439.
[16] Senthilkumar, S.; Vinodh, K.; Johnson Babu, G.; Gowtham, B. and Arulprakasam, V. (2019). Integrated seawater intrusion study of coastal region of Thiruvallur district, Tamil Nadu, South India. Applied Water Science, 9(5), 1-20.
[17] Ravikumar, P.; Prakash, K. L. and Somashekar, R. K. (2013). Evaluation of water quality using geochemical modeling in the Bellary Nala Command area, Belgaum district, Karnataka State, India. Carbonates and Evaporites, 28(3), 365-381.
[18] Appelo, C. A. J. and Postma, D. (1999). Variable dispersivity in a column experiment containing MnO2 and FeOOH-coated sand. Journal of contaminant hydrology, 40(2), 95-106.
[19] Embaby, A.; Razack, M.; Lecoz, M. and Porel, G. (2016). Hydrogeochemical assessment of groundwater in the Precambrian rocks, South Eastern Desert, Egypt. Journal of Water Resource and Protection, 8(03), 293-310.
[20] Hussain, T. A.; Almallah, I. A. and Al Qurnawi, W. S. (2021). Assessment of Dibdibba Groundwater Quality Using the Multivariate Statistical Technique in Zuber area South of Iraq. Iraqi Journal of Science, 2995-3008.
[21] Ewaid, S. H.; Mhajej, K. G.; Abed, S. A. and Al-Ansari, N. (2021, June). Groundwater Hydrochemistry Assessment of North Dhi-Qar Province, South of Iraq Using Multivariate Statistical Techniques. In IOP Conference Series: Earth and Environmental Science (Vol. 790, No. 1, p. 012075). IOP Publishing.
[22] Bahar, M. and Reza, M. (2010). Hydrochemical characteristics and quality assessment of shallow groundwater in a coastal area of Southwest Bangladesh. Environmental Earth Sciences, 61(5), 1065-1073.
[23] Bahrami, M.; Khaksar, E. and Khaksar, E. (2020). Spatial variation assessment of groundwater quality using multivariate statistical analysis (Case Study: Fasa Plain, Iran). Journal of Groundwater Science and Engineering Vol, 8(3), 230-243.
[24] Sajil Kumar, P. J. (2016). Deciphering the groundwater–saline water interaction in a complex coastal aquifer in South India using statistical and hydrochemical mixing models. Modeling Earth Systems and Environment, 2(4), 1-11.
[25] Rina, K.; Singh, C. K.; Datta, P. S.; Singh, N. and Mukherjee, S. (2013). Geochemical modelling, ionic ratio and GIS based mapping of groundwater salinity and assessment of governing processes in Northern Gujarat, India. Environmental earth sciences, 69(7), 2377-2391.
[26] Vengosh, A. and Rosenthal, E. (1994). Saline groundwater in Israel: its bearing on the water crisis in the country. Journal of Hydrology, 156(1-4), 389-430.
[27] Lekshmi, S. and Kani, M. K. (2017). Assessment of seawater intrusion using chemical indicators. Int. J. Eng. Adv. Technol, 7, 100-108.

[28] Moujabber, M. E.; Samra, B. B.; Darwish, T. and Atallah, T. (2006). Comparison of different indicators for groundwater contamination by seawater intrusion on the Lebanese coast. Water Resources Management, 20(2), 161-180.
[29] Todd, DK. (1959). Groundwater hydrology. United States. John Wiley and Sons. Inc.pp 277-294
[30] Kumar, P. J.; Elango, L. and James, E. J. (2014). Assessment of hydrochemistry and groundwater quality in the coastal area of South Chennai, India. Arabian Journal of Geosciences, 7(7), 2641-2653.
[31] Alfarrah, N. and Walraevens, K. (2018). Groundwater overexploitation and seawater intrusion in coastal areas of arid and semi-arid regions. Water, 10(2), 143.